P H Y S I C A L   R E V I E W   L E T T E R S

Waveguide-Based Off-Axis Holography with Hard X Rays

C. Fuhse, C. Ollinger, and T. Salditt

Institut für Röntgenphysik, Georg-August-Universität Göttingen, Friedrich-Hund-Platz 1, 37077 Göttingen, Germany
(Received 2 September 2006; published 21 December 2006)

We present an off-axis holography experiment based on the coherent cone beams emitted from a pair of x-ray waveguides. A magnified off-axis hologram is recorded, from which the phase of the optical transmission function of a sample is obtained by digital holographic reconstruction. A spatial resolution of about 100 nm has been achieved at 10.4 keV photon energy. Spatial resolution is determined by the cross-sectional dimensions of the waveguide and could approach a fundamental limit of about 10 nm in future experiments. In addition, we propose a new experimental setup that might overcome this limitation.

With increasing photon energy and a decreasing sample size, x-ray absorption decreases and matter mainly shifts the phase of x rays. The phase shift is proportional to the local electron density, which is encoded in the phase of x rays penetrating a sample. Since detectors are only sensitive to intensity, phase information has to be deduced from a measured intensity pattern. A variety of different techniques have been developed, like in-line phase-contrast imaging [1], coherent diffraction imaging [2–4], and various holographic techniques [5–9]. One-beam techniques like in-line holography or coherent diffraction imaging suffer from the loss of phase information. As a consequence, a straightforward holographic reconstruction from an in-line hologram is severely disturbed by the so-called twin image, and reconstruction from coherent diffraction data requires oversampling of the diffraction pattern and time-consuming iterative phase-retrieval algorithms [10]. The latter are often accompanied with problems concerning convergence of the algorithms and uniqueness of the solution.

The problem is overcome by two-beam techniques, where an additional reference beam probes the phase of the diffracted wave, enabling fast and unique reconstruction. In this sense, off-axis holography [11] is the two-beam extension of in-line holography, and Fourier transform holography [6,7] can be considered the two-beam extension of coherent diffraction imaging. Fourier transform holography has been carried out with soft x rays [6,7], and off-axis holography has been demonstrated in the hard x-ray regime with a prism beam splitter [9]. However, illumination with a split quasiparallel beam does not enable spatial resolution below the detector pixel size. A resolution of 40–50 nm was reported recording a hologram in a polymer photoresist [5], but fast and efficient detectors with sub-100 nm resolution are not available. On the contrary, illumination with divergent beams enables the recording of a magnified hologram, so that spatial resolution becomes practically independent from detector resolution [11]. Such a beam can be provided by focusing devices, or by waveguiding devices like glass capillaries [12] and

polymer channel waveguides [13,14]. The recording of a one-dimensionally magnified phase-contrast image (or in-line hologram) has already been demonstrated with a planar waveguide [15].

In this Letter we present an off-axis holography experiment using the mutual coherent cone beams emitted from a pair of x-ray channel waveguides. A magnified off-axis hologram is recorded, which enables fast and unique reconstruction. In the presented scheme the length of the waveguides can be adjusted in order to completely block background radiation in the cladding even for high photon energies. Compared to pinholes or slits which would ultimately also act as waveguides in the limit of high resolution [16], the lithographic fabrication enables additional optical design parameters. For example, we show that by using curved waveguides, the lateral distance between the two beams can be matched simultaneously to the lateral coherence length of the prefocusing optics and to the sample dimensions. The experimental setup is sketched in Fig. 1. A pair of coherently illuminated waveguides provides two mutual coherent cone beams. In the absence of a sample, this leads to the formation of a Young's fringe pattern on the detector. Introducing the sample, the pattern is modulated by the diffraction pattern of the sample. The phase of the diffracted wave shifts the fringes, while its amplitude changes the amplitude of the pattern. Thus both
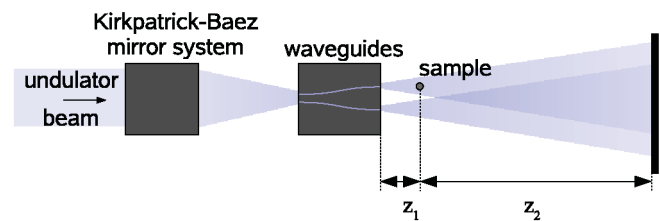
FIG. 1 (color). Experimental setup: An undulator beam is focused by Kirkpatrick-Baez mirrors and directly coupled into a pair of x-ray waveguides. One of the waveguides illuminates the sample while the other one provides an additional reference wave. A magnified off-axis hologram is recorded with a CCD camera. (Lengths and angles are not to scale.)

phase and amplitude of the diffracted wave are stored in the hologram. The recorded pattern corresponds to a magnified off-axis hologram, from which both phase and amplitude of the optical transmission function related to the sample can be obtained by digital holographic reconstruction. Magnification is the same as expected for a shadow image.

The recording of an in-line hologram with a waveguide is adequately described using the Fresnel-Kirchhoff diffraction formula. We use the paraxial approximation and consider the waveguide as a pointlike source. The spatial resolution of the imaging experiment is limited by the numerical aperture, which is here given by the divergence angle of the waveguide beam. For hard x rays, the latter is typically on the order of milliradians and limits spatial resolution to approximately the cross-sectional dimensions of the guiding core. It can be shown that a hologram recorded with a pointlike source is equivalent to a hologram that would be recorded with a parallel beam and the detector placed at the effective defocusing distance [15]

$$z_{\text{eff}} = \frac{z_1 z_2}{z_1 + z_2} \qquad (1)$$

downstream of the sample, where z_1 is the distance from the pointlike source to the sample and z_2 is the distance from the sample to the detector (Fig. 1). Compared to parallel beam illumination, the hologram is magnified by a factor

$$M = \frac{z_1 + z_2}{z_1}, \qquad (2)$$

which is the same as expected from ray optics. When a second cone beam is added as an additional reference wave, the recorded image becomes a magnified off-axis hologram. In one direction, the maximum field of view is then limited by the distance between the end faces of the waveguides, since larger objects cannot be fully illuminated without disturbing the reference beam. Reconstruction is carried out as follows: The recorded hologram is demagnified by the factor M and illuminated by a Gaussian reference beam. This leads to the formation of two first-order diffracted beams (Fig. 2): One contains the sample wave, which results in the formation of a focused image at distance z_{eff}. The other one contains the phase-conjugate wave, which results in the formation of a defocused twin image. The first-order beams include an angle

$$\theta_{\text{eff}} = \frac{d}{z_{\text{eff}}} \qquad (3)$$

with the reference beam, where d denotes the distance between the end faces of the waveguides [17]. For convenience, we chose a reference beam incident at an angle θ_{eff} from the appropriate direction to align the first-order beam providing the focused image along the optical axis. Applying scalar diffraction theory, the electric field amplitude in a plane directly downstream of the hologram is given by
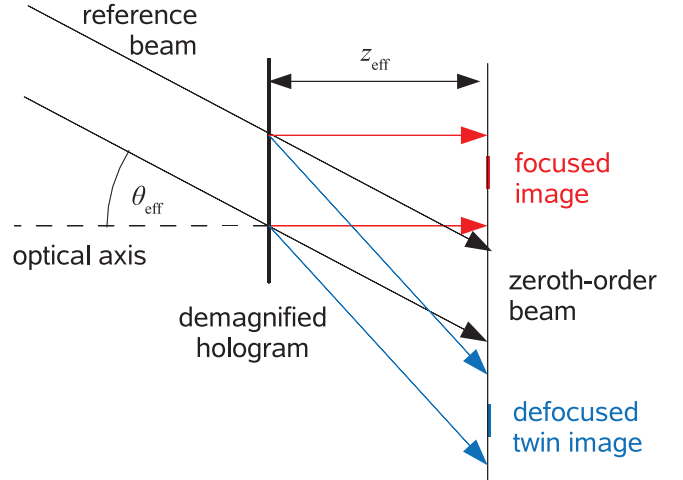
FIG. 2 (color). The recorded hologram is demagnified and illuminated by a Gaussian beam including an angle θ_{eff} with the optical axis. The underlying grating pattern (Young's fringes) creates two first-order beams. At the effective defocusing distance z_{eff} these beams create the focused image and a defocused twin image, respectively. (Lengths and angles are not to scale.)

$$E_1(x_1, y_1) = I_H(x_1, y_1) E_R(x_1, y_1), \qquad (4)$$

where $I_H(x_1, y_1)$ is the recorded intensity of the demagnified hologram and $E_R(x_1, y_1)$ denotes the amplitude of the Gaussian reference beam incident at an angle θ_{eff}. This field is propagated to a plane situated at the effective defocusing distance z_{eff}. The complex amplitude $E_2(x_2, y_2)$ in this plane is calculated using the Fresnel-Kirchhoff diffraction formula in the paraxial approximation

$$E_2(x_2, y_2) = \frac{\exp(ikz_{\text{eff}})}{i\lambda z_{\text{eff}}} \int E_1(x_1, y_1)$$
$$\times \exp\left(ik\frac{(x_2 - x_1)^2 + (y_2 - y_1)^2}{2z_{\text{eff}}}\right) dx_1 dy_1, \qquad (5)$$

where λ denotes the wavelength and k is the wave number in free space.

The waveguides used in the experiment consist of a polymer (calixarene, Allresist XAR-N7600/2) guiding core in Si [14]. The polymer was spin coated on a Si wafer and structured by means of electron beam lithography. A Leica LION LV 1 system was used, which is capable of writing Bezier curves with a length of several millimeters without stitching. A top Si cladding layer with a thickness of ≈ 200 nm was deposited by electron beam evaporation. The wafer was cleaved to a length of 4 mm, and the end faces of the waveguides were "polished" using a focused ion beam. The diameter of the guiding core is about 60 nm, and field calculations [18] indicate that the field at the end faces is dominated by the fundamental mode of approximately Gaussian shape.

The holography experiment was carried out at the ID22 undulator beam line of the European Synchrotron Radiation Facility in Grenoble (France). Photon energy was 10.4 keV, and the beam was focused by two perpendicularly crossed Kirkpatrick-Baez mirrors. The front faces of the waveguides were placed in the focal spot with cross-sectional dimensions of about $2.5 \times 5 \ \mu m^2$. The center-to-center distance between the front faces is 100 nm. Considering the focusing mirrors as an incoherent source, this corresponds to the transverse coherence length in the focal spot. However, a reasonable field of view requires a significantly larger spacing between the end faces. So the waveguides used here are slightly bent to increase the distance between the waveguides up to $d = 5 \ \mu m$ at the end faces. More precisely, the waveguides are parallel and straight over a length of ≈ 0.5 mm near the ends, while they are curved along two circular arcs on a total length of 3 mm in between. A larger spacing and field of view was prevented by the need to resolve the Young pattern with the CCD detector.

The holograms were recorded using a backilluminated CCD camera (Princeton Instruments PI-SX:1300, $20 \times 20 \ \mu m^2$ pixel size) placed 3.00 m downstream of the waveguides. Using this setup, we have imaged a small tungsten tip [Fig. 3(a)], which was prepared by standard techniques used in field ion microscopy [19]. The tip was placed at an effective defocusing distance of $z_{eff} \approx z_1 = 1.25$ mm, corresponding to a magnification of $M = 2400$. Exposure time was 30 s for each hologram.

Figure 3(b) shows a recorded hologram where the tip is placed in the center of the beam. The enlarged section shown in the inset resolves the underlying Young pattern. It could be expected that imperfections or misalignment of the waveguides may lead to an inhomogenous empty beam pattern, which must be taken into account by dividing the sample pattern by the empty beam. However, this was not necessary here. A holographic reconstruction was carried out and the phase of the reconstructed first-order beam, i.e.,
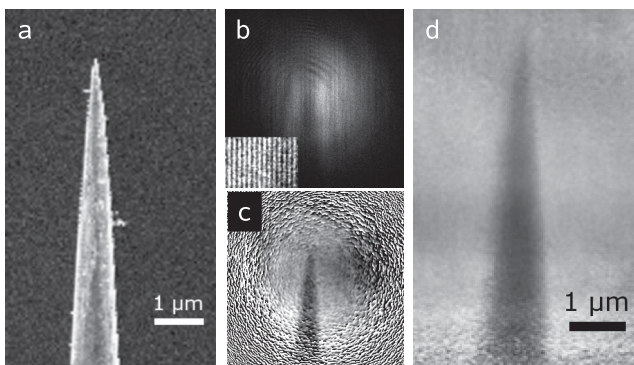
the phase of $E_2(x_2, y_2)$ as given in Eq. (5), is shown in Fig. 3(c). The shape of the tip is clearly recognized. Note that the noisy region is where intensity of the waveguide beam is practically zero. To increase the field of view, the sample was scanned in steps of 1 μm in both the horizontal and the vertical direction. Twenty-five holograms have been recorded at different positions. A superposition of the corresponding reconstructed waves yields the phase image shown in Fig. 3(d). The shape of the tip is clearly reproduced. The phase shift obtained from the reconstruction quantitatively matches the expected optical phase shift. This is verified by a comparison of the phase along slices through reconstructions to the calculated phase shift originating from a tungsten tip with a circular cross section, as shown in Fig. 4. A conservative estimate gives a spatial resolution of about 100 nm.

Identifying the numerical aperture of the imaging experiment with the divergence angle of the waveguide beam, we find that spatial resolution is limited to approximately the cross-sectional dimensions of the guiding core. Depending on the utilized materials, x rays may not be confined by waveguides to dimensions smaller than ≈ 10 nm [20]. This implies a fundamental limit for spatial resolution of the presented technique. To overcome this limit, it is necessary to access higher spatial frequencies corresponding to contributions of radiation scattered outside the waveguide cone beam [Fig. 5(a)]. One may therefore consider a modified reconstruction algorithm: Low spatial frequency contributions are obtained from holographic reconstruction, while high-frequency contributions are obtained using phase-retrieval algorithms evaluating the diffraction signal outside the waveguide cone beam as well. A similar approach as recently presented by Williams *et al.* could be used [4], and we anticipate that

FIG. 3. (a) Scanning electron microscopy image of the tungsten tip. (b) Recorded hologram. The magnified inset in the lower left shows the underlying Young pattern. (c) Phase of the reconstructed wave. (d) Phase image reconstructed from a superposition of 25 holograms recorded at different positions.
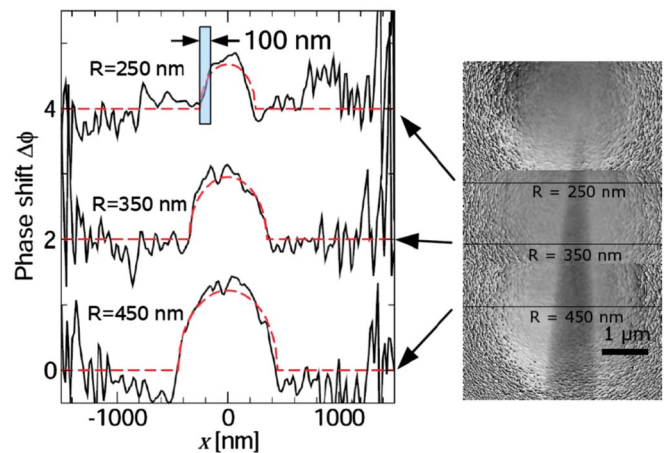
FIG. 4 (color). The reconstructed images of three individual holograms stitched together in order to increase the effective field of view. The phase shift along the indicated slices (solid black curves) is in good agreement with the phase shift calculated for a tungsten tip with a circular cross section and radii R (dashed red curves). From the edges of the tip we estimate that spatial resolution is about 100 nm.
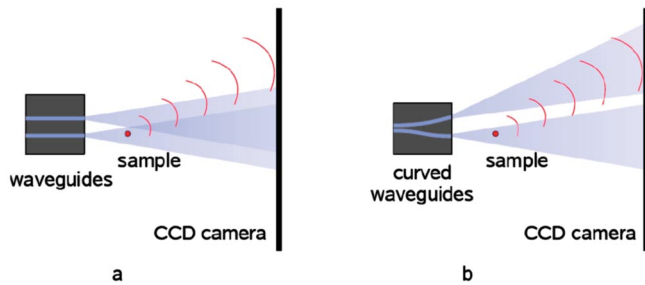
FIG. 5 (color). (a) Currently the divergence angle of the wave-guide cone beam determines the numerical aperture and thus spatial resolution. Higher spatial resolution requires the detection of radiation scattered outside the cone beam, but phase information is completely lost in the sketched setup. (b) Another appropriately curved waveguide could be applied to probe the phase of these contributions.

the additional reference wave can significantly improve reconstruction. The end faces of the waveguides (and a small region around it accounting for evanescent waves) provide a well-defined finite support. However, phase information could also be *directly measured* if a reference beam with a sufficiently large numerical aperture was available. This could be achieved by appropriately curved waveguides. As shown in Fig. 5(b), a curved waveguide could be applied to probe the phase in a limited region of reciprocal space, and multiple experiments with differently curved waveguides could successively probe reciprocal space in different directions.

In summary, x-ray waveguides have been used to record a magnified off-axis hologram, from which the complex optical transmission function of the sample is calculated by fast and nonrecursive numerical reconstruction. A quantitative phase image with a spatial resolution of about 100 nm was obtained in the present case. Current exposure times are on the order of several seconds and could be further reduced by applying more efficient focusing mirrors. With the availability of x-ray free-electron lasers [21], single-shot exposures will be feasible, providing about 100 fs temporal resolution. Calculations show that the transmission of monomodal waveguides can be increased to $T \geq 50\%$, if the overexposure ratio σ (prefocusing spot/ waveguide cross section) is decreased to $\sigma \leq 1000$, and if the polymer is replaced by air in the waveguide core [16]. Importantly, the method is well suited for tomography. Because of the small numerical aperture in the order of milliradians, the focal depth is between 2 and 3 orders of magnitude larger than lateral spatial resolution. This, in principle, enables high-resolution three-dimensional imaging of comparably large volumes. Spatial resolution of the presented technique is approximately given by the cross-sectional dimensions of the guiding core. Higher resolution requires an increased numerical aperture, which can

probably be realized by means of appropriately curved waveguides.

[1] P. Cloetens, R. Barrett, J. Baruchel, J.-P. Guigay, and M. Schlenker, J. Phys. D **29**, 133 (1996).
[2] J. Miao, P. Charalambous, J. Kirz, and D. Sayre, Nature (London) **400**, 342 (1999).
[3] H. N. Chapman *et al.*, J. Opt. Soc. Am. A **23**, 1179 (2006).
[4] G. J. Williams, H. M. Quiney, B. B. Dhal, C. Q. Tran, K. A. Nugent, A. G. Peele, D. Paterson, and M. D. de Jonge, Phys. Rev. Lett. **97**, 025506 (2006).
[5] M. Howells, C. Jacobsen, J. Kirz, R. Feder, K. McQuaid, and S. Rothman, Science **238**, 514 (1987).
[6] I. McNulty, J. Kirz, C. Jacobsen, E. H. Anderson, M. R. Howells, and D. P. Kern, Science **256**, 1009 (1992).
[7] S. Eisebitt, J. Lüning, W. F. Schlotter, M. Lörgen, O. Hellwig, W. Eberhardt, and J. Stöhr, Nature (London) **432**, 885 (2004).
[8] N. Watanabe, K. Sakurai, A. Takeuchi, and S. Aoki, Appl. Opt. **36**, 7433 (1997).
[9] Y. Kohmura, T. Sakurai, T. Ishikawa, and Y. Suzuki, J. Appl. Phys. **96**, 1781 (2004).
[10] R. J. Fienup, Opt. Lett. **3**, 27 (1978).
[11] E. N. Leith, J. Upatnieks, and K. A. Haines, J. Opt. Soc. Am. **55**, 981 (1965).
[12] D. H. Bilderback, S. A. Hoffman, and D. J. Thiel, Science **263**, 201 (1994).
[13] F. Pfeiffer, C. David, M. Burghammer, C. Riekel, and T. Salditt, Science **297**, 230 (2002).
[14] A. Jarre, C. Fuhse, C. Ollinger, J. Seeger, R. Tucoulou, and T. Salditt, Phys. Rev. Lett. **94**, 074801 (2005).
[15] S. Lagomarsino, A. Cedola, P. Cloetens, S. D. Fonzo, W. Jark, S. Souillié, and C. Riekel, Appl. Phys. Lett. **71**, 2557 (1997).
[16] C. Fuhse and T. Salditt, Opt. Commun. **265**, 140 (2006).
[17] Ignoring the sample, this is easily seen from a comparison of the Young pattern of two mutually coherent pointlike source to the cosine grating pattern resulting from interference of coherent parallel beams.
[18] C. Fuhse and T. Salditt, Appl. Opt. **45**, 4603 (2006).
[19] R. B. Doak, Y. Ekinci, B. Holst, J. P. Toennies, T. Al-Kassab, and A. Heinrich, Rev. Sci. Instrum. **75**, 405 (2004).
[20] C. Bergemann, H. Keymeulen, and J. F. van der Veen, Phys. Rev. Lett. **91**, 204801 (2003).
[21] J. Feldhaus, J. Arthur, and J. B. Hastings, J. Phys. B **38**, S799 (2005).